Designing Yang–Mills Topological Vacua with Cold Atoms

Shi-Liang Zhu(朱诗亮)[1,2,3*]

[1]*Key Laboratory of Atomic and Subatomic Structure and Quantum Control (Ministry of Education), School of Physics, South China Normal University, Guangzhou 510006, China*
[2]*Guangdong Provincial Key Laboratory of Quantum Engineering and Quantum Materials, South China Normal University, Guangzhou 510006, China*
[3]*Quantum Science Center of Guangdong-Hong Kong-Macao Greater Bay Area, Shenzhen 518000, China*

(Received 15 December 2025; accepted manuscript online 16 March 2026)

Topological vacua, a family of degenerate ground states of the Yang–Mills fields with zero field strength but nontrivial topological structures, play a fundamental role in particle physics and quantum field theory. However, they have not yet been experimentally observed. Here, we propose an experimental scheme to realize a real-space $SU(2)$ artificial Yang–Mills topological vacua using a cloud of two-Λ-level cold atoms. We derive analytical expressions for the gauge transformations and gauge potentials of these topological vacua. Specifically, we propose a degenerate subspace that supports Yang–Mills gauge fields and identify the laser configurations required to realize the topological vacua. Furthermore, we generalize the vacua to a family with a topological number given by the product of two integers. We also propose an Aharonov–Bohm interference experiment to detect the resulting geometric phases, which persist even with vanishing gauge field strengths throughout space, distinct from the electromagnetic case.

DOI: 10.1088/0256-307X/43/4/040602 CSTR: 32039.14.0256-307X.43.4.040602

Introduction. The vacuum of a gauge field is a field state with zero field strength and is crucial to our understanding of some remarkable features of particle physics and quantum fields.[1,2] In electromagnetic fields, the vanishing field strength results in the only choice of a vanishing gauge potential. In contrast, the non-Abelian Yang–Mills field is predicted to have an intriguing type of topological vacua, namely, a family of degenerate ground states with zero field strength but nonzero gauge potentials, and each state is characterized by a topological number.[2–5] This type of vacua is fundamentally different from an Abelian vacuum in terms of energy degeneracy and field topology. Furthermore, quasiparticles called instantons are known to describe the tunneling processes between different vacua, enabling the introduction of the CP-violating θ term and providing insights into the mechanism of quark confinement.[1,2] However, these nonperturbative solutions of the Yang–Mills fields, first proposed in 1975,[3] have not yet been experimentally observed.

Recently, artificial gauge fields have been extensively studied for cold atoms[6,7] and other quantum-engineered systems.[8,9] Artificial Abelian and non-Abelian gauge fields have been theoretically proposed[10–14] and experimentally realized in various configurations of the laser-atom interactions.[15–23] Some quantum field models, such as the Higgs model and Dirac monopoles, have been realized using cold atoms or Bose–Einstein condensates.[24–27] In these studies, the Yang–Mills topological vacua have also been simulated with a Λ-level configuration in a Bose–Einstein condensate.[22] However, they exist only in parameter space, rather than in real spatial space, and the laser structure required for realizing topological vacua in real space is complicated and challenging to implement. This largely limits further investigation; for example, some of the crucial features of the Yang–Mills topological vacua, such as the real-space Aharonov–Bohm effects and instantons, cannot be explored with the gauge fields in parameter space. Therefore, the quantum engineering community must identify an experimentally feasible laser-atom configuration to realize real-space topological vacua.

In this study, we propose an experimental scheme to realize real-space $SU(2)$ artificial Yang–Mills topological vacua using a cloud of two-Λ-level cold atoms coupled with four laser fields. First, we analytically obtain explicit expressions for the gauge transformations of Yang–Mills topological vacua to analyze their geometric and topological features. Then, we identify two degenerate eigenstates for the atoms in a two-Λ-level configuration coupled with four laser fields. These two degenerate states form a subspace that can support the $SU(2)$ Yang–Mills gauge field. Notably, we demonstrate that this system is suitable for realizing Yang–Mills topological vacua. In addition, we confirm that two conventional configurations (tripod-level[6,10,13] and triangle-level[28] configurations), which are capable of supporting Yang–Mills gauge fields, are inapplicable for topological vacua. Inspired by lasers requiring an orbital angular momentum of one, we generalize this type of topological vacua to a novel family of topological vacua characterized by a topological number nl, where the integer n is the original topological num-

*Corresponding author. Email: slzhu@scnu.edu.cn
© 2026 Chinese Physical Society and IOP Publishing Ltd. All rights, including for text and data mining, AI training, and similar technologies, are reserved.

ber, and l denotes orbital angular momentum. In recent years, numerous investigations of non-Abelian Aharonov–Bohm effects[29–40] have been reported, and the key noncommutative properties of non-Abelian gauge fields have been experimentally observed.[31–40] However, the persistence of a nontrivial phase effect, even when the gauge field strengths are exactly zero everywhere—a key and more counterintuitive feature of the Yang–Mills case—has been rarely experimentally explored. This phenomenon represents a fundamental distinction between the electromagnetic Aharonov–Bohm and Yang–Mills effects. To observe this fundamental effect, we propose an Aharonov–Bohm interference experiment for topological vacua.

Three-Dimensional $SU(2)$ Yang–Mills Topological Vacua. We first recall the basic idea of the $SU(2)$ Yang–Mills topological vacua.[3–5] The Lagrangian density for the Yang–Mills theory in Minkowski space is given by $\mathcal{L} = (1/2g^2)\mathrm{tr}(F_{\mu\nu}F^{\mu\nu})$, where g is the gauge coupling constant, $F_{\mu\nu} = \partial_\mu A_\nu - \partial_\nu A_\mu - \mathrm{i}[A_\mu, A_\nu]$ is the field strength tensor, and A_μ is a gauge potential. The vacuum states are defined under the condition that the field strength vanishes ($F_{\mu\nu} = 0$). The solutions to this condition are pure gauge configurations: $A_\mu = \mathrm{i}U^{-1}(\boldsymbol{r})\partial_\mu U(\boldsymbol{r})$, where $\boldsymbol{r} = (x, y, z)$ is the position vector, and $U(\boldsymbol{r})$ is a map from three-dimensional space to the gauge group $SU(2)$. To obtain finite energy, we require $F_{\mu\nu} \to 0$ at spatial infinity ($r = |\boldsymbol{r}| \to \infty$). This compactifies space into a three-sphere S^3. Thus, we consider maps $U(\boldsymbol{r})$ from S^3 (space) to S^3 ($SU(2)$ group manifold). These maps are classified by the homotopy group $\pi_3(S^3) = \mathbb{Z}$, and each map is characterized by an integer $n \in \mathbb{Z}$ called the winding number or Pontryagin index. An explicit representation of a map with the winding number n is[3]

$$U_n(\boldsymbol{r}) = \left(\frac{r^2 - \eta^2}{r^2 + \eta^2}\sigma_0 - \frac{2\mathrm{i}\eta\boldsymbol{r}\cdot\boldsymbol{\sigma}}{r^2 + \eta^2}\right)^n, \tag{1}$$

where η is a constant, and hereafter, we assume $\eta = 1$; $\boldsymbol{\sigma} = (\sigma_x, \sigma_y, \sigma_z)$ are Pauli matrices, and σ_0 is the identity matrix. Evidently, field strength $F_{\mu\nu}$ related to the gauge transformation U_n vanishes, and thus, these configurations represent degenerate vacua.

An analytical expression can facilitate further exploration of system properties. A rigorous method for deriving an explicit expression for U_n is presented in the Supplemental Material.[41] In spherical coordinates $\{r, \theta, \varphi\}$, equation (1) can be rewritten as

$$U_n = \frac{1}{(r^2+1)^n}[(r^2 - 1)\sigma_0 - 2\mathrm{i}r\sigma_\mathrm{r}]^n,$$

where σ_r is the radial Pauli matrix defined as $\sigma_\mathrm{r} = \hat{\boldsymbol{r}}\cdot\boldsymbol{\sigma} = \begin{pmatrix} \cos\theta & \sin\theta\mathrm{e}^{-\mathrm{i}\varphi} \\ \sin\theta\mathrm{e}^{\mathrm{i}\varphi} & -\cos\theta \end{pmatrix}$ with $\hat{\boldsymbol{r}} = \boldsymbol{r}/r$. Using the binomial expansion

$$U_n = \frac{1}{(r^2+1)^n}\sum_{k=0}^{n} C_n^k (r^2-1)^{n-k}(-2\mathrm{i}r)^k \sigma_\mathrm{r}^k,$$

and property $\sigma_\mathrm{r}^2 = \sigma_0$, we obtain the following explicit expression:

$$U_n = \cos(2n\alpha)\sigma_0 + \mathrm{i}\sin(2n\alpha)\sigma_\mathrm{r}, \tag{2}$$

where $\alpha = \arctan(r)$, and the total sign $(-1)^n$ is omitted. This result can be used to design laser configurations for implementing topological vacua.

These vacua $|n\rangle$ are connected by nonperturbative solutions called instantons. An instanton is a finite-action solution in Euclidean spacetime and interpolates between the $n = 0$ vacuum at $t = -\infty$ and the $n = 1$ vacuum at $t = +\infty$. In quantum theory, tunneling effects lead to a superposition of these topological states, resulting in the formation of the θ-vacuum. The angle θ is a fundamental parameter of the theory and leads to nonperturbative effects such as CP violation.

Realizing Topological Vacua with Atoms. Herein, we demonstrate our approach for realizing topological vacua with artificial gauge fields in cold atoms. The Hamiltonian for a laser–atom interaction system is $H = (\boldsymbol{p}^2/2m) + V(\boldsymbol{r}) + H_\mathrm{AL}$, where m is the atomic mass, H_AL is an $N \times N$ matrix in the basis of internal energy levels $|j\rangle$, and $V(\boldsymbol{r}) = \sum_{j=1}^{N} V_j(\boldsymbol{r})|j\rangle\langle j|$ is an external potential. The full quantum state can be expanded to $|\Phi(\boldsymbol{r})\rangle = \sum_{j=1}^{N}\phi_j(\boldsymbol{r})|j\rangle$. The system can be represented in the basis of dressed states $|\chi_n(\boldsymbol{r})\rangle$, which is defined as the eigenvectors of H_AL satisfying $H_\mathrm{AL}|\chi_n\rangle = \varepsilon_n|\chi_n\rangle$. In this basis, the full quantum state is expressed as $|\tilde{\Phi}(\boldsymbol{r})\rangle = \sum_j \psi_j(\boldsymbol{r})|\chi_j(\boldsymbol{r})\rangle$. The wave function in the dressed basis, $|\tilde{\Psi}\rangle = (|\psi_1\rangle, |\psi_2\rangle, \ldots, |\psi_N\rangle)^{\mathcal{T}}$ (where $\mathcal{T}$ denotes the transpose), obeys the Schrödinger equation $\mathrm{i}\hbar(\partial/\partial t)|\tilde{\Psi}\rangle = \tilde{H}_\mathrm{eff}|\tilde{\Psi}\rangle$. The effective Hamiltonian is $\tilde{H}_\mathrm{eff} = U_\mathrm{T}^\dagger H U_\mathrm{T}$, and the transformation matrix is defined as $|\Phi(\boldsymbol{r})\rangle = U_\mathrm{T}|\Psi(\boldsymbol{r})\rangle$.

We further assume that the first J dressed states are degenerate and energetically well-separated from the remaining $N - J$ states to project the full Hamiltonian onto this J-dimensional subspace. Then, the wave function in the subspace, $|\Psi\rangle = (|\psi_1\rangle, |\psi_2\rangle, \ldots, |\psi_J\rangle)^{\mathcal{T}}$, satisfies the Schrödinger equation $\mathrm{i}\hbar(\partial/\partial t)|\Psi\rangle = H_\mathrm{eff}|\Psi\rangle$, with the effective Hamiltonian taking the form:[10,11,42–44]

$$H_\mathrm{eff} = \frac{1}{2m}(-\mathrm{i}\hbar\nabla - \boldsymbol{A})^2 + V_\mathrm{eff}. \tag{3}$$

Here, $\boldsymbol{A} = \mathrm{i}\hbar U_\mathrm{A}^\dagger \nabla U_\mathrm{A}$, where U_A is a $J \times J$ matrix in U_T. The scalar potential V_eff is a $J \times J$ matrix with elements $(V_\mathrm{eff})_{n,m} = (1/2m)\sum_{l=J+1}^{N} \boldsymbol{A}_{n,l}\cdot\boldsymbol{A}_{l,m}$. This term is typically small because it is second order in the gauge potentials and can often be omitted; moreover, it can be compensated for by additional laser fields if necessary.

Artificial $SU(2)$ Yang–Mills gauge fields can be realized using ultracold atoms with two fully (or nearly) degenerate states by designing laser-atom interactions. Two degenerate states can be achieved with a tripod-level[6,10,13] or triangle-level[28] configuration. However, we examined these two configurations and did not find suitable laser forms for realizing topological vacua. Here, we demonstrate that a two-Λ-level configuration can support $SU(2)$ Yang–Mills gauge fields and that it can be used to realize real-space $SU(2)$ topological vacua.

We consider a cloud of two-Λ-level atoms coupled by four lasers with Rabi frequencies $\Omega_{1,2,3,4}$, as shown in

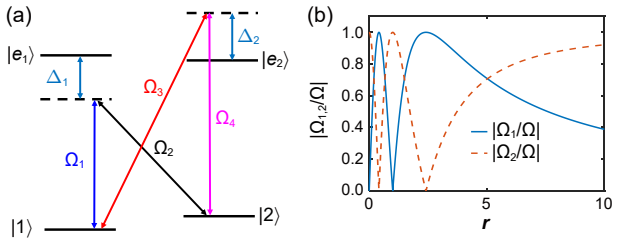

Fig. 1. Energy-level configuration and Rabi frequencies for topological vacua. (a) Two-Λ-type system, under the conditions $\omega_1+\omega_4=\omega_2+\omega_3$, $\Omega_1=\Omega_3$, $\Omega_2=\Omega_4$, and $\Delta_1=-\Delta_2=-\Delta$, yielding two degenerate eigenstates that form subspaces for the SU(2) Yang–Mills gauge field. (b) Rabi frequencies $|\Omega_{1,2}|$ required for a topological vacuum with a topological number $n=2$.

Fig. 1(a). Under the condition $\omega_1+\omega_4=\omega_2+\omega_3$, the Hamiltonian $H_{\rm AL}$ in the basis $\{|1\rangle,|2\rangle,|e_1\rangle,|e_2\rangle\}$ can be written as[41]

$$H_{\rm AL}=\frac{\hbar}{2}\begin{pmatrix}0&0&\Omega_1^*&\Omega_3^*\\0&0&\Omega_2^*&\Omega_4^*\\\Omega_1&\Omega_2&2\Delta_1&0\\\Omega_3&\Omega_4&0&2\Delta_2\end{pmatrix},\tag{4}$$

where $\Delta_{1,2}$ are laser detunings. Solving the Schrödinger equation $H_{\rm AL}|\chi\rangle=\epsilon|\chi\rangle$, we observe that the system has two degenerate eigenstates with $\epsilon=0$ under the following conditions: $\Omega_1=\Omega_3$, $\Omega_2=\Omega_4$, and $\Delta_1=-\Delta_2=-\Delta$. In this case, the other two eigenvalues are given by $\epsilon=\pm(\hbar/2)\sqrt{4\Delta^2+2\Omega^2}$, where $\Omega=\sqrt{|\Omega_1|^2+|\Omega_2|^2}$. The two degenerate eigenstates for $\epsilon=0$ can be obtained as

$$|\chi_1\rangle=\begin{pmatrix}\Omega_2\\-\Omega_1\\0\\0\end{pmatrix},\quad |\chi_2\rangle=\begin{pmatrix}\Omega_1^*\\\Omega_2^*\\\dfrac{\Omega^2}{2\Delta}\\-\dfrac{\Omega^2}{2\Delta}\end{pmatrix}.$$

For a large detuning $|\Delta|\gg\Omega$, the population in both the $|e_1\rangle$ and $|e_2\rangle$ states is extremely small and can be neglected; thus, we can restrict our analysis to the subspace $\{|1\rangle,|2\rangle\}$. Under this condition, the normalized wave functions for $\epsilon=0$, in the basis $\{|1\rangle,|2\rangle\}$, are given by

$$|\chi_1\rangle=\frac{1}{\Omega}\begin{pmatrix}\Omega_2\\-\Omega_1\end{pmatrix},\quad |\chi_2\rangle=\frac{1}{\Omega}\begin{pmatrix}\Omega_1^*\\\Omega_2^*\end{pmatrix}.$$

The transformation matrix for the effective Hamiltonian in Eq. (3) is

$$U_{\rm A}=\frac{1}{\Omega}\begin{pmatrix}\Omega_2^*&\Omega_1\\-\Omega_1^*&\Omega_2\end{pmatrix}.\tag{5}$$

A comparison with the vacuum solutions of the gauge transformation U_n described in Eq. (2), we find that a three-dimensional topological vacuum with topological number n is realized when the Rabi frequencies are given by

$$\Omega_1(\boldsymbol{r})=\mathrm{i}\Omega\sin\theta\sin(2n\alpha)\mathrm{e}^{-\mathrm{i}\varphi},\tag{6}$$

$$\Omega_2(\boldsymbol{r})=\Omega[\cos(2n\alpha)-\mathrm{i}\cos\theta\sin(2n\alpha)].\tag{7}$$

Two-Dimensional SU(2) Yang–Mills Topological Vacua. Conducting experimental investigations of the topological vacua is fundamentally important. One potential method for realizing the laser configurations described by Eqs. (6) and (7) involves using a spatial light modulator and high-numerical-aperture aspheric lens to create the three-dimensional spatial structure of lasers.[45] However, a full three-dimensional implementation is challenging. As an initial yet crucial step, we explore the feasibility of realizing lower-dimensional topological vacua. Inspired by this idea and the three-dimensional topological vacua of $SU(2)$ Yang–Mills fields,[3–5] we have investigated a family of two-dimensional topological vacua described by the gauge transformations $U_n=(U_1)^n$, where

$$U_1=\frac{1}{r^2+1}\begin{pmatrix}r^2-1&-2\mathrm{i}r\mathrm{e}^{-\mathrm{i}\varphi}\\-2\mathrm{i}r\mathrm{e}^{\mathrm{i}\varphi}&r^2-1\end{pmatrix}.\tag{8}$$

Here, we use two-dimensional polar coordinates (r,φ). The analytical expression for $U_n=(U_1)^n$ is derived in[41]

$$U_n=\begin{pmatrix}\cos(2n\alpha)&\mathrm{i}\mathrm{e}^{-\mathrm{i}\varphi}\sin(2n\alpha)\\\mathrm{i}\mathrm{e}^{\mathrm{i}\varphi}\sin(2n\alpha)&\cos(2n\alpha)\end{pmatrix},\tag{9}$$

where the total sign $(-1)^n$ is omitted. The corresponding gauge potentials $A_\mu=iU_n^{-1}\partial_\mu U_n$ are given by

$$A_\varphi=-\sin(2n\alpha)[\sin(2n\alpha)\sigma_z+\cos(2n\alpha)\sigma_\varphi],\tag{10}$$

where the Pauli matrix along the φ-direction is $\sigma_\varphi=\hat{\varphi}\cdot\boldsymbol{\sigma}=\begin{pmatrix}0&-\mathrm{i}\mathrm{e}^{-\mathrm{i}\varphi}\\\mathrm{i}\mathrm{e}^{\mathrm{i}\varphi}&0\end{pmatrix}$, and

$$A_r=-\frac{2n}{r^2+1}\sigma_{\rm r}(\theta=\pi/2),\tag{11}$$

where $\sigma_{\rm r}(\theta=\pi/2)=\begin{pmatrix}0&\mathrm{e}^{-\mathrm{i}\varphi}\\\mathrm{e}^{\mathrm{i}\varphi}&0\end{pmatrix}$. We can verify that $F_{r\varphi}=F_{\varphi r}=0$, where the field strength is defined as $F_{\mu\nu}\equiv\partial_\mu A_\nu-\partial_\nu A_\mu-\mathrm{i}[A_\mu,A_\nu]$.

For a gauge group G with the gauge field $A_\mu(x)=A_\mu^a(x)T^a$ (here, the group generators are $T^a=\sigma_{\rm r},\sigma_\varphi$), the topological properties are characterized by a Wilson loop along a closed path C:

$$\Gamma_{\rm C}=\mathcal{P}\exp\left(\mathrm{i}\oint_{\rm C}A_\mu(x)\mathrm{d}x^\mu\right),\tag{12}$$

where $\mathcal{P}$ denotes path ordering. The physical meaning can be illustrated by considering loops at fixed r. In this case, we obtain

$$\Gamma_r=\mathcal{P}\exp\left(\mathrm{i}\oint_{\rm C}A_\varphi\mathrm{d}\varphi\right)=\mathrm{e}^{-\mathrm{i}\gamma(r)\sigma_z},\tag{13}$$

where the phase is expressed as

$$\gamma(r)=2\pi\sin^2\left[2n\arctan(r)\right].\tag{14}$$

The function $\gamma(r)$ exhibits n maxima at positions $r_m=\tan[(2m-1)\pi/4n]$ for $m=1,\ldots,n$, with each maximum reaching $\gamma_{\rm Max}(r_m)=2\pi$. It also exhibits $n+1$ minima: n discrete minima at $r_k=\tan(k\pi/2n)$ for $k=0,\ldots,n-1$, where $\gamma_{\rm Min}(r_k)=0$, and an additional asymptotic minimum at $r\to\infty$. Figure 2 shows the phases $\gamma(r)$ obtained

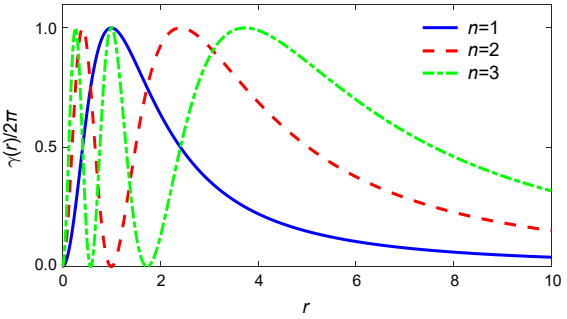

Fig. 2. Geometric phases $\gamma(r)$ in Eq. (14) for $n = 1, 2, 3$.

from Eq. (14) for $n = 1, 2, 3$. In topological terminology, a closed path with a geometric phase of 2π corresponds to a winding number of one. Therefore, the topological number n of these two-dimensional vacua manifests as the existence of n distinct radial positions r_m, at which the Wilson loop attains a unit winding number.

A comparison with the vacuum solutions of the gauge transformation U_n described in Eq. (9) reveals that a topological vacuum with a topological number n can be realized if the Rabi frequencies adopt the following forms:

$$\Omega_1(\boldsymbol{r}) = \mathrm{i}\Omega \mathrm{e}^{-\mathrm{i}\varphi} \sin(2n\alpha), \quad \Omega_2(\boldsymbol{r}) = \Omega \cos(2n\alpha). \tag{15}$$

As a typical example, the values of $|\Omega_{1,2}/\Omega|$ for $n = 2$ are presented in Fig. 1(b). The $\mathrm{e}^{-\mathrm{i}\varphi}$ term in Eq. (15) can be realized using the lasers Ω_1 and Ω_3 carrying an orbital angular momentum of one.

New Family of Topological Vacua Inspired by Their Realization. Notably, equation (15) suggests that a topological vacuum can be realized when the lasers Ω_1 and Ω_3 carry an orbital angular momentum of one. Following this result, we examine the phenomenon occurring when these lasers have an orbital angular momentum l. In this case, the factor $\mathrm{e}^{\mathrm{i}\varphi}$ in Eq. (9) is replaced with $\mathrm{e}^{\mathrm{i}l\varphi}$, and thus, the phase $\gamma(r)$ in Eq. (14) becomes

$$\gamma(r) = 2l\pi \sin^2 \left[2n \arctan(r)\right]. \tag{16}$$

The spatial positions of the maxima and minima, as expressed in Eq. (14), remain unchanged. However, the value of the phases at the maximum becomes $\gamma(r_m) = 2l\pi$.

This type of solution for topological vacua can also be generalized in three dimensions. We define

$$U_1^{(l)} = \frac{1}{r_+^2} \begin{pmatrix} r_-^2 - 2\mathrm{i}r\cos\theta & 2\mathrm{i}r\mathrm{e}^{-\mathrm{i}l\varphi} \\ 2\mathrm{i}r\mathrm{e}^{\mathrm{i}l\varphi} & r_-^2 + 2\mathrm{i}r\cos\theta \end{pmatrix}, \tag{17}$$

in the spherical coordinates $\{r, \theta, \varphi\}$, where $r_\pm^2 = r^2 \pm 1$. Denoting $U_n^{(l)} = (U_1^{(l)})^n$ and $A_\mu^{(n,l)} = U_n^{(l)} \partial_\mu (U_n^{(l)})^{-1}$, the topological number characterizing the vacua described by Eq. (17) is given by

$$N_n^{(l)} = \frac{1}{24\pi^2} \int \epsilon_{ijk} \mathrm{tr}(A_i^{(n,l)} A_j^{(n,l)} A_k^{(n,l)}) \mathrm{d}^3x = nl. \tag{18}$$

Thus, we obtain a new family of three-dimensional vacua with the topological number nl. In two dimensions, such vacua can be realized using lasers with orbital angular momentum l, which provides an alternative method for realizing topological vacua with arbitrary integer topological numbers.

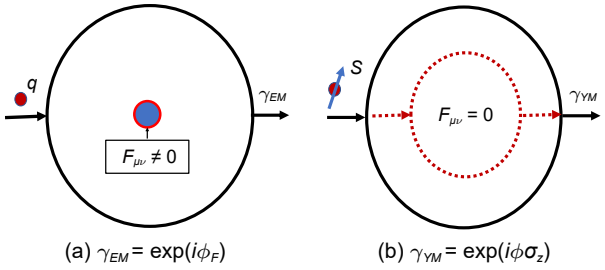

Fig. 3. Comparison of geometric phases: the Aharonov–Bohm effect in electromagnetism versus that in SU(2) Yang–Mills topological vacua. (a) Electromagnetic Aharonov–Bohm effect: A charged particle q traversing a closed path acquires a geometric phase $\exp(\mathrm{i}\phi_F)$, where $\phi_F = (q/\hbar) \int F_{\mu\nu}\, \mathrm{d}^2\boldsymbol{x}$. This phase is nonzero only if the magnetic flux is enclosed within the path. (b) Aharonov–Bohm effect in a Yang–Mills topological vacuum: A spin-1/2 particle circling at a fixed radius r acquires a phase γ_{YM} in the matrix form $\exp(\mathrm{i}\phi\sigma_z)$. Remarkably, the phase factor ϕ can be nonzero even when the field strength $F_{\mu\nu}$ vanishes everywhere in space. Furthermore, the acquired phase depends on the radius r.

Comparison of the Electromagnetic and Yang–Mills Aharonov–Bohm Effects. The geometric phase[42,43] in Eq. (12) [and Eq. (14)] can be detected via Aharonov–Bohm type interference experiments. Therefore, comparing the electromagnetic Aharonov–Bohm effect with the Yang–Mills Aharonov–Bohm effect yields intriguing outcomes.

As illustrated in Fig. 3, an Aharonov–Bohm phase $\exp(\mathrm{i}\phi)$ with a phase factor $\phi = q\Phi_F/\hbar$ arises when the particle traverses a closed path enclosing the magnetic flux Φ_F. The magnetic flux is defined as $\Phi_F = \oint \boldsymbol{A} \cdot \mathrm{d}\boldsymbol{l} = \int \boldsymbol{B} \cdot \mathrm{d}\boldsymbol{S}$, where $\boldsymbol{B} = \nabla \times \boldsymbol{A}$ is the magnetic flux density. A nonvanishing ϕ appears even when the particle moves in a region where the electromagnetic fields are zero, provided that the vector potential $\boldsymbol{A}$ is nonzero. This result demonstrates that electromagnetic potentials are physically significant in quantum mechanics. However, the nonzero phase factor ultimately depends on the nonvanishing magnetic flux (i.e., a nonzero magnetic field within the area enclosed by the particle's path). This geometric phase manifests in interference experiments even when the particles experience zero local fields, highlighting the nonlocal role of the magnetic flux. Thus, the Aharonov–Bohm effect underpins fundamental studies in quantum physics, revealing profound connections between gauge potentials and quantum phases.

The Schrödinger-like equation with $SU(2)$ gauge coupling, which describes the quantum mechanics of a nonrelativistic spin-1/2 particle interacting with an SU(2) Yang–Mills field, is given by

$$\mathrm{i}\hbar \frac{\partial}{\partial t} |\psi\rangle = \left[\frac{1}{2m}(\nabla - \mathrm{i}gA^a\sigma^a)^2 + gA_0^a\sigma^a\right] |\psi\rangle. \tag{19}$$

We consider the $SU(2)$ Yang–Mills field proposed in our experimental scheme; it is a vacuum field with a topological number n, and the corresponding gauge potentials A_φ and A_r are given by Eqs. (10) and (11), respectively. In this case, a general matrix-valued phase

$$\Gamma_{\rm C} = \mathcal{P}\exp\left[\mathrm{i}\oint_{\rm C}(A_\varphi \mathrm{d}\varphi + A_r \mathrm{d}r)\right] \tag{20}$$

is observed. If the path of the atoms is a circle of a fixed radius r, as shown in Fig. 3, then it accumulates a phase $\mathrm{e}^{-\mathrm{i}\gamma(r)\sigma_z}$ with $\gamma(r) = 2\pi\sin^2[2n\arctan(r)]$. The proposed geometric phases can be observed through Aharonov–Bohm interference experiments.

The Yang–Mills and electromagnetic Aharonov–Bohm effects differ in two key aspects: (1) the noncommutativity of the Yang–Mills gauge fields, which has been experimentally reported in various quantum systems;[31–40] and (2) an observable phase emerges even when the gauge field strengths are identically zero everywhere in space. This second, more counterintuitive feature remains unexplored both theoretically and experimentally. These results indicate that the Yang–Mills Aharonov–Bohm interference proposed here, based on a two-Λ-level configuration, can be realized, and the resulting remarkable geometric phases can be observed. Thus, both distinctive features can be investigated simultaneously in our proposed cold-atom experiment.

Conclusion. In this study, we proposed an experimental scheme to realize topological vacua in real space using cold atoms and explored their nontrivial properties. The Aharonov–Bohm effect induced by the Yang–Mills topological vacua is observable even when the gauge field strengths are zero throughout the space; this feature fundamentally distinguishes the Yang–Mills topological vacua-induced Aharonov–Bohm effect from the electromagnetic Aharonov–Bohm effect. Our theoretical proposal may stimulate further experimental studies in the near future. The realization of topological vacua in real space will enable the examination of various long-pursued phenomena, including instantons, the CP-violating θ term, quark confinement, and axions (a potential dark matter candidate), via tabletop experiments.[46–51]

Acknowledgments. The work was supported by the National Key Research and Development Program of China (Grant No. 2022YFA1405300), the Innovation Program for Quantum Science and Technology (Grant No. 2021ZD0301705), and Guangdong Provincial Quantum Science Strategic Initiative (Grant No. GDZX2304-002).

References

[1] Weinberg S 1996 *The Quantum Theory of Fields* (Cambridge University Press)
[2] Bick E and Steffen F D 2005 *Topology and Geometry in Physics* (Springer-Verlag)
[3] Belavin A, Polyakov A, Schwartz A, and Tyupkin Y 1975 *Phys. Lett. B* **59** 85
[4] 't Hooft G 1976 *Phys. Rev. Lett.* **37** 8
[5] Jackiw R and Rebbi C 1976 *Phys. Rev. Lett.* **37** 172
[6] Zhang D W, Zhu Y Q, Zhao Y X, Yan H, and Zhu S L 2018 *Adv. Phys.* **67** 253
[7] Dalibard J, Gerbier F, Juzeliunas G, and Ohberg P 2011 *Rev. Mod. Phys.* **83** 1523
[8] Tan X, Zhang D W, Zheng W, Yang X, Song S, Han Z, Dong Y, Wang Z, Lan D, Yan H, Zhu S L, and Yu Y 2021 *Phys. Rev. Lett.* **126** 017702
[9] Chen M, Li L, Palumbo P, Zhu Z, Goldman G, and Cappellaro C 2022 *Science* **375** 1017
[10] Ruseckas J, Juzeliūnas G, Ohberg P, and Fleischhauer M 2005 *Phys. Rev. Lett.* **95** 010404
[11] Zhu S L, Fu H, Wu C J, Zhang S C, and Duan L M 2006 *Phys. Rev. Lett.* **97** 240401
[12] Li Y, Bruder C, and Sun C P 2007 *Phys. Rev. Lett.* **99** 130403
[13] Zhu S L, Zhang D W, and Wang Z D 2009 *Phys. Rev. Lett.* **102** 210403
[14] Zhu S L, Shao L B, Wang Z D, and Duan L M 2011 *Phys. Rev. Lett.* **106** 100404
[15] Lin Y J, Compton R L, Perry A R, Phillips W D, Porto J V, and Spielman I B 2009 *Phys. Rev. Lett.* **102** 130401
[16] Beeler M C, Williams R A, Jimenez-Garcia K, LeBlanc L J, Perry A R, and Spielman I B 2013 *Nature* **498** 201
[17] Duca L, Li T, Reitter M, Bloch I, Schleier-Smith M, and Schneider U 2015 *Science* **347** 288
[18] Wu Z, Zhang L, Sun W, Xu X T, Wang B Z, Ji S C, Deng Y, Chen S, Liu X J, and Pan J W 2016 *Science* **354** 83
[19] Huang L, Meng Z, Wang P, Peng P, Zhang X L, Chen L, Li D, Zhou Q, and Zhang J 2016 *Nat. Phys.* **12** 540
[20] Kolkowitz S, Bromley S L, Bothwell T, Wall M L, Marti G E, Koller A P, Zhang X, Rey A M, and Ye J 2017 *Nature* **542** 66
[21] Lv Q X, Du Y X, Liang Z T, Liu H Z, Liang J H, Chen L Q, Zhou L M, Zhang S C, Zhang D W, Ai B Q, Yan H, and Zhu S L 2021 *Phys. Rev. Lett.* **127** 136802
[22] Li J Z, Zou C J, Du Y X, Lv Q X, Huang W, Liang Z T, Zhang D W, Yan H, Zhang S C, and Zhu S L 2022 *Phys. Rev. Lett.* **129** 220402
[23] Lv Q X, Liu H Z, Du Y X, Chen L Q, Wang M, Liang J H, Fu Z X, Chen Z Y, Yan H, and Zhu S L 2023 *Phys. Rev. A* **108** 023316
[24] Ray M W, Ruokokoski E, Kandel S, Möttönen M, and Hall D S 2014 *Nature* **505** 657
[25] Yang B, Sun H, Ott R, Wang H Y, Zache T, Halimeh J, Yuan Z S, Hauke P, and Pan J W 2020 *Nature* **587** 392
[26] Leonard J, Morales A, Zupancic P, Donner T, and Esslinger T 2017 *Science* **358** 1415
[27] Endres M, Fukuhara T, Pekker D, Cheneau M, Schaub P, Gross C, Demler E, Kuhr S, and Bloch I 2012 *Nature* **487** 454
[28] Du Y X, Liu B J, Lv Q X, Zhang X D, Yan H, and Zhu S L 2017 *Phys. Rev. A* **96** 012333
[29] Yang Y, Yang B, Ma G, Li J, Zhang S, and Chan C T 2024 *Science* **383** adf9621
[30] Zhai D W and Yao W 2020 *Phys. Rev. Lett.* **125** 266404
[31] Liang Q, Dong Z, Pan J S, Wang H, Li H, Yang Z, Yi W, and Yan B 2024 *Nat. Phys.* **20** 1738
[32] Wu J, Wang Z, Biao Y, Fei F, Zhang S, Yin Z, Hu Y, Song Z, Wu T, Song F, and Yu R 2022 *Nat. Electron.* **5** 635
[33] Dong Z, Wu X, Yang Y, Yu P, Chen X, and Yuan L 2024 *Nat. Commun.* **15** 7392
[34] Yang Y, Peng C, Zhu D, Buljan H, Joannopoulos J D, Zhen B, and Soljacic M 2019 *Science* **365** 1021
[35] Chen Y, Zhang R Y, Xiong Z, Hang Z H, Li J, Shen J Q, and Chan C T 2019 *Nat. Commun.* **10** 3125
[36] Leroux F, Pandey K, Rehbi R, Chevy F, Miniatura C, Gremaud B, and Wilkowski D 2018 *Nat. Commun.* **9** 3580
[37] Cheng D, Wang K, Roques-Carmes C, Lustig E, Long O Y, Wang H, and Fan S 2025 *Nature* **637** 52

[38] Sun Y K, Shan Z L, Tian Z N, Chen Q D, and Zhang X L 2024 *Nat. Commun.* **15** 9311
[39] Shan Z L, Sun Y K, Tao R, Chen Q D, Tian Z N, and Zhang X L 2024 *Phys. Rev. Lett.* **133** 053802
[40] Neef V, Pinske J, Klauck F, Teuber L, Kremer M, Ehrhardt M, Heinrich M, Scheel S, and Szameit A 2023 *Nat. Phys.* **19** 30
[41] See Supplemental Materials for the derivation of Eqs. (2) and (9) and the Hamiltonian in Eq. (4).
[42] Berry M V 1984 *Proc. A* **392** 45
[43] Wilczek F and Zee A 1984 *Phys. Rev. Lett.* **52** 2111
[44] Sun C P and Ge M L 1990 *Phys. Rev. D* **41** 1349
[45] Barredo D, Lienhard V, de Leseleuc S, Lahaye T, and Browaeys A 2018 *Nature* **561** 79
[46] Borsanyi S, Fodor Z, Guenther J, Kampert K H, Katz S D, Kawanai T, Kovacs T G, Mages S W, Pasztor A, Pittler F, Redondo J, Ringwald A, and Szabo K K 2016 *Nature* **539** 69
[47] Kharzeev D E and Levin E M 2015 *Phys. Rev. Lett.* **114** 242001
[48] Kang Z B and Kharzeev D E 2011 *Phys. Rev. Lett.* **106** 042001
[49] Dziarmaga J, Rams M M, and Zurek W H 2022 *Phys. Rev. Lett.* **129** 260407
[50] Klinkhamer F R and Volovik G E 2022 *Phys. Rev. D* **105** 084066
[51] Chen S, Ievlev E, and Shifman M 2025 *Proc. Natl. Acad. Sci. U.S.A.* **122** e2502703122